A Biomechatronic Extended Physiological Proprioception (EPP) Controller for Upper-Limb Prostheses

Anestis Mablekos-Alexiou, *Student Member, IEEE*, Georgios A. Bertos, *Member, IEEE,* and
Evangelos Papadopoulos, *Senior Member, IEEE*

Abstract—We propose a biomechatronics-based master/slave topology which is going to provide an Extended Physiological Proprioception (EPP)-equivalent control but without the use of a harness, cineplasty, or Bowden cable. The proposed control uses an implanted micro servo actuator. The original Bowden-cable EPP topology is compared to the proposed one and their simulation results are presented. The simulation results are encouraging since they indicate the materialization potential of the topology, both in terms of control and of low power, two essential factors in making the presence of an implant in the human body feasible. This control topology will provide a modern EPP-equivalent control scheme for upper-limb prostheses without the disadvantages of previous EPP configurations but with the control advantages of proprioceptive feedback.

I. INTRODUCTION

The replacement of a human hand or arm is a truly challenging task. Any prosthesis is constrained by volume, it must be light in weight, and if an external power source is used it must operate at low power [1], [2]. However, these are not the most daunting aspects of the challenge. The major hurdle to be overcome is the problem of control. The following attributes have been presented as desirable for prosthesis control: low mental loading or subconscious control, simple to learn to use, independence in multifunctional control, parallel control, speed of response, maintaining the integrity of human functional ability and natural appearance [2], [3].

Extended Physiological Proprioception (EPP) topology first noted by Simpson D.C. in 1974 [4] as a control scheme for upper-limb prostheses, is superior to velocity control and myoelectric control due to the direct mapping of position, velocity and force between the residual limb and the prosthesis [5]. EPP can best be thought of as the extension of the operator's proprioception into the prosthesis, that is, the prosthesis becomes an extension of the amputee's self [1]. This leads to subconscious control - one of the desirable attributes of prosthesis needs [2, 3] - and it is valuable for multi-functional prostheses [4]. EPP can be implemented via

different schemas: harness and cables (which is troublesome for the user), cineplasty [6-12] or exteriorized tendons [13] plus cables which is again aesthetically unacceptable by the user and requires post-amputation surgery. It is evident that the disadvantages of EPP (post-amputation surgical procedures of cineplasty or exteriorized tendons, Bowden cables, aesthetics) have led to the sole adaptation of myoelectric control after its introduction in the 1960s by Kobrisnski of the USSR Academy of Sciences [14]. The problem is though that together with the disadvantages of EPP, the advantages of it (i.e. subconscious control) also vanished. There was some activity of funded research in the field of EPP but without commercial adoption. Weir et al. [15] fitted a below-elbow amputee with an externally powered hand using his exteriorized tendons cineplasties as control inputs to an analog EPP controller previously developed at Northwestern University Prosthetics Research Laboratory (Fig. 1), [16]. Bertos et al. [17, 18] designed in the same Laboratory a one degree-of-freedom (DoF) microprocessor based EPP controller to overcome the limitations of this original analog controller. Al-Angari et al. [19] expanded the above-mentioned EPP controller to a 2-DoFs controller. Both of these controllers are battery-powered using force command input and either a harness or Bowden cables for the EPP linkage.

Control of prostheses, airplanes, automobiles and remote manipulators had similar evolution in their early years. In all of them there was a direct physical connection/mechanical linkage between the user and the device which made the operator "feel" where the device was. However, prosthetics later diverged from the others with the use of myoelectric control which is an open loop control scheme where vision compensates for the lack of proprioceptive feedback [17]. The user lacks subconscious sensory feedback of the state of the prosthesis and therefore control of many Degrees of Freedom (DoFs) is almost impossible.

As airplanes got bigger, hydraulic power assist was added to to the cable controls. Aircraft controls borrowing from the field of remote manipulators have gone away from the direct physical interconnection of pilot and flight surfaces and now use fly-by-wire systems which still preserve the operator proprioceptive feedback ("feel"). Fly-by-wire systems have been inspired by Goertz [20] at Argonne who built the first bilateral force reflecting master slave remote manipulator for handling radioactive material. Later on, Mosher [21] at

General Electric built a force reflecting manipulator with power augmentation. In these systems, the user is connected to the flight surfaces via electrical wires or sensors and the systems use bilateral master slave techniques with force feedback to provide the operator with the appropriate "feel".
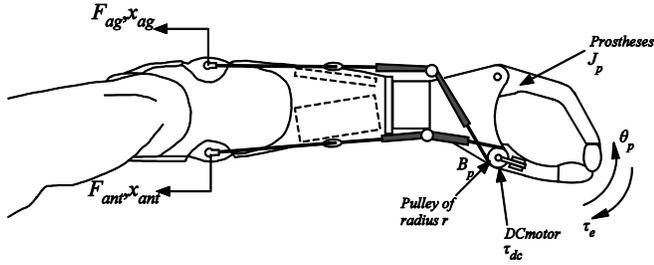
Figure 1: Classic EPP control topology (Adapted from [18]).

II. SYSTEM MODELING

A. System Model for Classic EPP

The dynamics of a bidirectional, single Dof Bowden cable prosthesis system, see Fig. 1, is modeled as an inertia with friction:

$$J_p \ddot{\theta}_p + B_p \dot{\theta}_p + K_p \theta_p = \tau_{dc} + \tau_{mu} + \tau_e \qquad (1)$$

where θ_p denotes angular position of the prosthetic hand; J_p, B_p and K_p denote the equivalent inertia, viscous coefficient and stiffness of the system, respectively and τ_e is the torque exerted on the prosthesis by its environment. The curvature effect of the Bowden cable is insignificant, therefore can be disregarded and the Coulomb friction of the system is negligible as the prosthesis is supported by bearings. The DC motor torque, τ_{dc}, is proportional to the torque applied by the co-contraction of both agonist and antagonist muscles τ_{mu}, and it can be written as follows

$$\tau_{dc} = G_{bc} \tau_{mu} = G_{bc} \left(F_{ag} - F_{ant} \right) r \qquad (2)$$

where G_{bc} is the muscles' torque gain in the case of prosthesis control via Bowden cable, r is the pulley radius, F denotes force, and subscript 'ag' and 'ant' denote the agonist and antagonist muscle, respectively (Fig. 1).
Thus, (1) transforms to

$$J_p \ddot{\theta}_p + B_p \dot{\theta}_p + K_p \theta_p = \left(1 + G_{bc}\right)\left(F_{ag} - F_{ant}\right) r + \tau_e \qquad (3)$$

Assuming that, in the whole range of the prosthetic's movement, the moment arms of the antagonist pair of muscles are constant and opposite to each other, then the position of each muscle's cable is described by

$$\begin{cases} x_{ag} = r \cdot \theta_p \\ x_{ant} = -r \cdot \theta_p \end{cases} \qquad (4)$$

where x denotes position.

B. System Model for Biomechatronic EPP

In this paper, we propose a technologically biomechatronics inspired architecture which provides a functionally subconscious control scheme for prosthesis control (Fig. 2) inherent in the classic EPP topology (Fig. 1), but without its inherent disadvantages of wires and aesthetics. There is a master implanted module which is interfaced to the commanding muscles via force sensors. There is also a slave module (external prosthesis). The implanted module is charged via inductive coupling. The master and slave module are coupled in a master/slave topology.
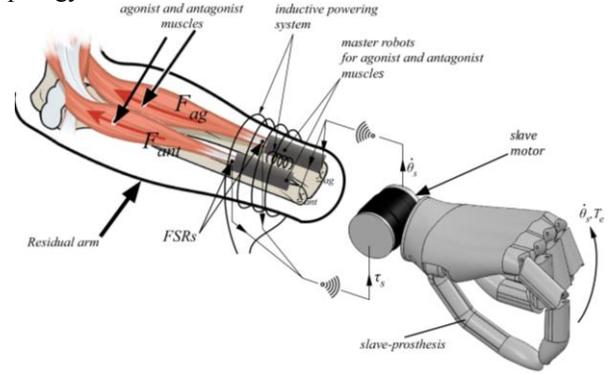
Figure 2: Proposed Biomechatronic EPP-equivalent control topology.

Thus, instead of using a Bowden cable, EPP can be implemented to some extent via a teleoperation system, where each muscle of the antagonistic pair is attached to the end effector of a low power master robot applying direct forces to it. Hence, the length/velocity of each muscle is controlled by the corresponding master DC motor and follows the slave DC motor of the prosthesis faithfully guaranteeing the transparency of the teleoperation system (Fig. 2), [22].

B.1 Slave Robot Modeling

The slave robot corresponds to the prosthesis, and as with the case of control via Bowden cable, it can be modeled as

$$J_p \ddot{\theta}_s + B_p \dot{\theta}_s + K_p \theta_s = \tau_s + \tau_e \qquad (5)$$

where θ_s is the angular position of the slave and τ_s is the torque applied to the prostheses by the slave DC motor.

B.2 Master Robot Modeling

Each master robot is a micro servo which converts the rotary motion of a DC motor into linear via a lead screw drive. In a system like this, modeling of the transmission is important both in terms of achieving satisfactory control as well as accurate power estimation, since the intense friction phenomena affect both of these factors.

In Fig. 3, a screw spiral with its nut extends along a surface. The guide enables the nut to travel in linear motion preventing its rotation. The Static-plus-Kinetic friction model, which is given by (6), is used to describe the physics of the solid-to-solid contact between screw and nut,

$$T_f = \begin{cases} T_C \, \mathrm{sgn}\, \dot{\theta}, \dot{\theta} \neq 0 \\ T_e, |T_e| < T_s, \dot{\theta} = 0, \ddot{\theta} = 0 \\ T_s \, \mathrm{sgn}\, T_e, |T_e| > T_s, \dot{\theta} = 0, \ddot{\theta} \neq 0 \end{cases} \qquad (6)$$

where T_e is the total external torque, T_C is the Coulomb friction torque, T_s is the breakaway torque, and $\dot{\theta}$ is the

sliding velocity between the surfaces.

As shown in Fig. 3, λ is the lead angle of the screw, m is the mass of the nut, J_m is the total inertia, B_m is the dynamic viscous coefficient of the DC motor and the screw support bearings, τ_m is the torque applied to the screw by the motor, d the major diameter of the screw, and p the screw pitch.

Figure 3: Extended screw spiral and nut.

Fig. 3 shows analysis of the forces, in case muscle force F_{mu} has the same direction as nut velocity. Assuming that N_1 is the normal force to the helix with pressure angle θ_n, N_2 is the normal force to the nut's guide, and μ denotes the coefficient of Coulomb friction then the friction forces between the surfaces are given below:

$$\left\{ \begin{array}{l} F_{fs} = \mu N_1 \\ F_{fn} = \mu \left| N_2 \right| = F_{fs} \cos \lambda - N_1 \cos \theta_n \sin \lambda \end{array} \right\} \quad (7)$$

where, F_{fs} is the tangent to the helix friction force and F_{fn} is the friction force between the nut and the guide. The screw dynamics is given by:

$$J_m \ddot{\theta}_m + B_m \dot{\theta}_m = \tau_m + \frac{d}{2} N_1 \left(\cos \theta_n \sin \lambda - \mu \cos \lambda \right) \quad (8)$$

For the nut dynamics, considering that N_1 has its reactive counterpart $\left(-N_1 \right)$, we have:

$$m \ddot{x}_n = F_{mu} - F_{fn} - N_1 \left(\cos \theta_n \cos \lambda + \mu \sin \lambda \right) \quad (9)$$

The kinematic relation between the screw and the nut is:

$$x_n = \tan \lambda \frac{d}{2} \theta_m = \frac{p}{2\pi} \theta_m \quad (10)$$

where θ_m is the angular displacement of the screw and x_n is the linear displacement of the nut. Equations (6), (7), (8), (9) can be combined and by elimination of the normal force, we have the system's dynamics:

$$J_m \ddot{\theta}_m + B_m \dot{\theta}_m = \tau_m - \underbrace{\frac{\frac{d}{2} \cdot \xi_1}{\mu \cdot \xi_1 + 1}}_{C_1} F_{mu} + \underbrace{\frac{\left(\frac{d^2}{2} \right) \cdot \tan \lambda \cdot \xi_1 \cdot m}{\mu \cdot \xi_1 + 1}}_{J_1} \ddot{\theta}_m \quad (11)$$

where $\xi_1 = \dfrac{\mu \cos \lambda - \cos \theta_n \sin \lambda}{\cos \theta_n \cos \lambda + \mu \sin \lambda}$.

Performing a similar analysis for the instances where force F_{mu} has the opposite direction from velocity $\dot{x}_n$ or $F_{mu} = 0$ then we come to the following equation of motion:

$$J_m \ddot{\theta}_m + B_m \dot{\theta}_m = \tau_m - \tau_f \quad (12)$$

where τ_f is given below for each individual case:

- if F_{mu} has the same direction as $\dot{x}_n$, then

$$\tau_f = C_1 \cdot F_{mu} - J_1 \ddot{\theta}_m \quad (13)$$

- if F_{mu} has the opposite direction as $\dot{x}_n$, then

$$\tau_f = -C_2 \cdot F_{mu} + J_2 \cdot \ddot{\theta}_m \quad (14)$$

- if $F_{mu} = 0$, then

$$\tau_f = J_2 \cdot \ddot{\theta}_m \quad (15)$$

where the coefficients $\xi_1, \xi_2, C_1, C_2, J_1, J_2$ are functions of the screw parameters and are given in the Appendix. The parameters of the master system including an off-the-shelf 1.5W DC motor and a lead screw assembly are shown in Table I. Finally, the parameters of the prosthesis are given below, in Table II.

TABLE I
MASTER SYSTEM PARAMETERS

Symbol	Name	Value	Unit
B_m	Viscous coefficient	1.05e-6	Nms/rad
J_m	Inertia	1.34e-7	kgm^2
d	Screw diameter	3.6e-3	mm
p	Screw pitch	1.22e-3	mm
μ_s	Static friction coefficient	0.12	-
μ_k	Kinetic friction coefficient	0.09	-

TABLE II
PROSTHESIS-SLAVE PARAMETERS

Symbol	Name	Value	Unit
B_p	Viscous coefficient	0.15	Nms/rad
K_p	Stiffness coefficient	0.4	Nm/rad
J_p	Inertia	4e-3	kgm^2
r	Moment arm	1.5e-2	m

B.3 Delayed Signals and Scaling Factors

The proposed bilateral teleoperation system, controlled by a position-force (P-F) architecture, is shown in Fig. 4. Assuming that the communication delay is constant and equal to T_d, the signals from and to the communication block are related as:

$$\left\{ \begin{array}{l} F_{ag}^d (t) = F_{ag} \left(t - T_d \right) \\ F_{ant}^d (t) = F_{ant} \left(t - T_d \right) \end{array} \right\} \quad (16)$$

$$\theta_s^d (t) = \theta_s \left(t - T_d \right) \quad (17)$$

where F_{ag}^d, F_{ant}^d the delayed force signals from agonist and antagonist muscle respectively and θ_s^d the delayed position signal from the prosthesis.

Using appropriate scaling factors, the torque command to the slave and the position command to the master are modified such that:

$$\begin{cases} x_{n,ag} = G_p \theta_s^d \\ x_{n,ant} = -G_p \theta_s^d \end{cases} \tag{18}$$

$$\tau_s = G_f r \left(F_{ag}^d - F_{ant}^d \right) \tag{19}$$

where $x_{n,ag}, x_{n,ant}$ denote the nut position of agonist and antagonist master robots and G_p, G_f are the position and force scaling factors, respectively.
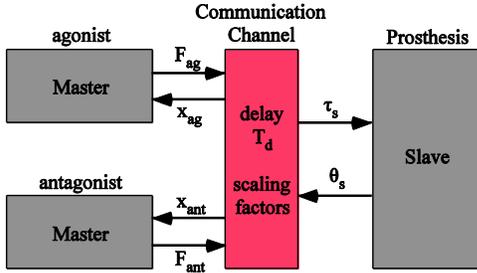
Figure 4: Master/Slave communication network.

III. CONTROL DESIGN

A. Force tracking control of the slave

Torque control of the slave is achieved by modulating its DC motor current. The dynamics of the prosthesis become as follows:

$$J_p \ddot{\theta}_s + B_p \dot{\theta}_s + K_p \theta_p = G_f \left(F_{ag}^d - F_{ant}^d \right) r + \tau_e \tag{20}$$

Combining (3) and (19) gives the appropriate force scaling factor so that, in the case of a Biomechatronic EPP, torque of the prosthesis is similar to the one of a Classic EPP for the same forces exerted by the muscles:

$$G_f = \left(1 + G_{bc} \right) \tag{21}$$

Ideal force tracking can be achieved with the absence of signal transportation delay.

B. Position tracking control of the master

A Proportional-Derivative law controls the screw angular displacements in order to set the position for each nut. Thus, for each muscle's implanted master DC motor the rotors' desired position θ^{des} is:

$$\begin{cases} \theta_{m,ag}^{des} = r\theta_s^d \dfrac{2}{d \cdot \tan \lambda} \\ \theta_{m,ant}^{des} = -r\theta_s^d \dfrac{2}{d \cdot \tan \lambda} \end{cases} \tag{22}$$

The control diagram of the master is represented in Fig. 5. The nonlinear friction is modeled as a feedback to the linear dynamics, K_P and K_V are simple gains and k_t is the DC motor torque constant. Then, the closed loop error dynamics with $e = \theta_m^{des} - \theta_m$ is:

$$\ddot{e} + \frac{B_m + K_V k_t}{J_m} \dot{e} + \frac{K k_t}{J_m} e = \ddot{\theta}_m^{des} + \frac{B_m + K_P k_t}{J_m} \dot{\theta}_m^{des} + \frac{1}{J_m} \tau_f \tag{23}$$

Thus, the natural frequency ω_n and the damping ratio ζ of the system are given below:

$$\omega_n = \left(\frac{K_P k_t}{J_m} \right)^{\frac{1}{2}} \tag{24}$$

$$\zeta = \frac{\left(B_m + K_V k_t \right)}{2\omega_n \cdot J_m} \tag{25}$$
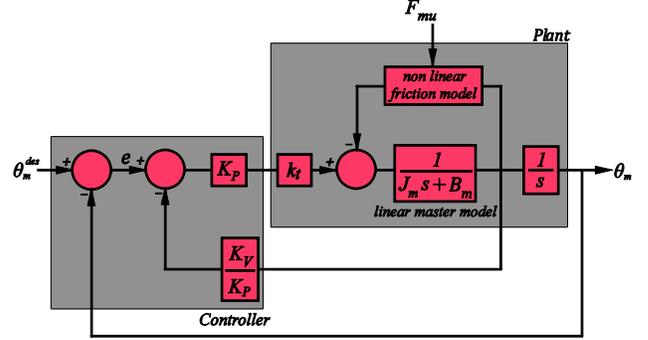
Figure 5: PD controller for each of the master actuators.

The gain K_P is selected in a way that enables us to have a quick response and thereafter using K_V we set the damping at $\zeta = 0.707$. Thus, for the desired settling time $t_s = 4/\zeta\omega_n = 0.002s$ the set of gains is selected as $K_P = 253.2$ and $K_V = 0.12$.

IV. SIMULATION RESULTS

System control was performed using the models that were developed in MATLAB/Simulink. The purpose of the comparisons made through simulations for the Classic EPP and the Biomechatronic EPP, is to evaluate the proposed topology both in terms of transparency and feasibility. The approach that was used to determine transparency was the position-force approach which defines transparency based on simultaneous position and force tracking of the master and slave [22].

To demonstrate the system's performance, we conducted a simulation run where three fundamental types of the human muscle-joint functions were executed (Fig. 6). In these types, the neural signal which constitutes the input, is converted into muscular activation/deactivation, and ultimately into muscle force which is a length/velocity function of the contractile element. The models used, which are highly nonlinear, were proposed by Winters and Stark [23], [24] and refer to antagonist muscles of the wrist, where each of the two muscles exerts maximum isometric force equal to 100N.

More specifically, in the $0 - 0.5s$ interval, an isometric pulse response, which arises from simultaneous maximal co-contraction of the antagonistic muscles, was simulated. In an isometric muscle function the input is the neural signal, while the joint velocity is set to zero. Then, in the $0.5 - 1s$ interval, an anisometric (free) pulse response was simulated. In this case, the neural signal for the agonist muscle is a pulse function reaching 50% of its maximal value, and since the

antagonist muscle is idle and the external load is zero, the prosthesis can move. Finally, in the $1-2.5s$ interval a neutrally-initiated sinusoidal movement was performed, by placing neural inputs to the antagonistic muscles out of phase.

It must be noted that an $1.5W$ DC servomotor, was assumed to drive each master lead screw, with a voltage and current saturation of $3V$ and $2A$, respectively. This power was calculated to be necessary so that the master robot of each muscle could follow the prosthesis throughout all the aforementioned function cases. Force scaling factor in the case of Classic EPP, G_{bc} was chosen equal to 1.5 whereas in the case of Biomechatronic EPP, $G_f = 2.5$. The amount of time delay in the communication channels was set to $0.005s$.

The simulated neural signal is shown in Fig. 6a and the forces ensuing from it in Fig. 6b. Fig. 7 and Fig. 8 display the results of the controlled mechanical energy variables of the proposed teleoperation system (Biomechatronic EPP), compared to the respective energy variables of the Classic EPP. Those results reveal adequate transparency of the system, particularly when regarding to the negligible dissimilarity in position response between the implanted master robot and Bowden cable (Fig. 9a, Fig. 9c), something necessary for the muscles to give accurate information to the amputee about the position of the prosthesis. On the other hand, the muscle forces amplification, which occurs necessarily in order to maintain the power demands at reasonable levels, does not provoke significant degradation of transparency for two reasons. First of all, the muscles of an amputee are already of lower capacity than the ones of a normal person, which makes scaling up necessary anyway and secondly, because neuroplasticity will help the amputee to get familiar with the physical change.

Figure 7: Real (black dashed-line) and amplified amount of torque for the Classic EPP (red dashed-line) and Biomechatronic EPP (black line) cases.
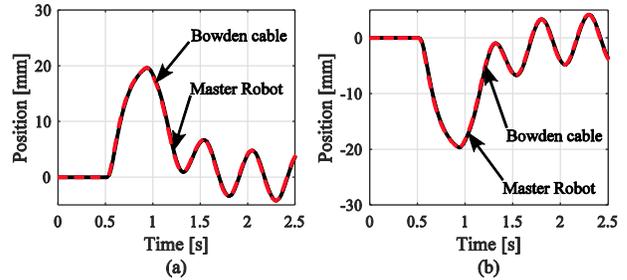
Figure 8: (a) Bowden cable and master robot position response for agonist muscle, (b) Bowden cable and master robot position response for antagonist muscle.
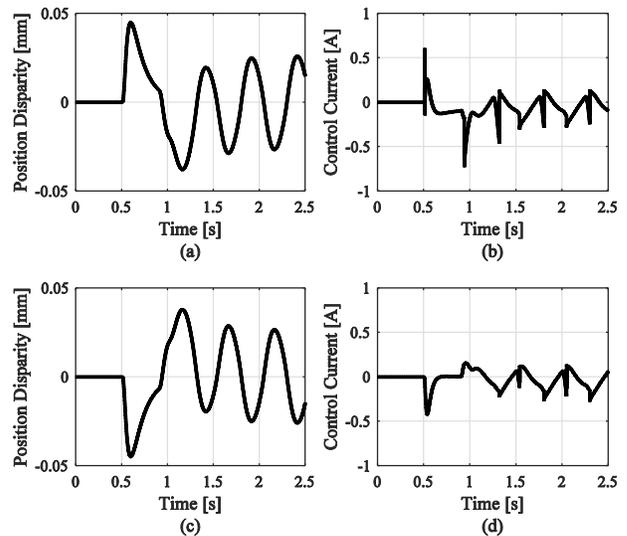
Figure 9: (a), (c) difference in position response between Bowden cable and master robot for agonist and antagonist muscles, (b), (d) control current of each master DC motor.

Figure 6: (a) Neural signals for agonist (black line) and antagonist (red dashed-line) muscles, (b) Muscles' applied forces.
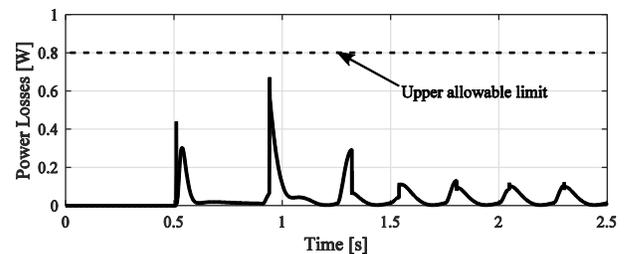
Figure 10: Total power losses of the implantable motorized lead-screw assemblies.

Finally, an initial feasibility analysis which was performed for all the components of the topology set the 0.8W as the upper allowable limit for the total power losses of the implantable motorized master lead-screws [25]. The results given in Fig. 10, indicate the viability of the functional existence of the proposed system in the human body, while, at the same time, accommodating the fundamental functions of the human upper-limbs that were simulated.

V. CONCLUSION

We feel that the key to successful control of multi-joint prostheses is subconscious sensory feedback. We believe that EPP and EPP controllers applied to externally-powered prostheses is a viable approach of achieving multi-functional control. The presented initial simulation results show adequate equivalency of the Classic and Biomechatronic EPP topologies in order to move to the next step of validation with a future physically implemented biocompatible Biomechatronic EPP prototype. In addition, initial feasibility calculations have been performed with positive results for a charging method for the implant of inductive coupling and using low power Bluetooth for data transmission between the Master and the Slave modules [25]. We believe that the proposed topology can be more acceptable to perspective users due to the fact that aesthetically unpleasant Bowden cables and cineplastic surgical procedures will not be needed any more. A surgical procedure will be needed to connect the master mechanism to the musculature, but this can be very well performed at the time of amputation. The proposed Biomechatronic EPP topology could function in the future as a building block of many DoFs prosthetic systems with superior control.

APPENDIX

The coefficients of the (13), (14), and (15) are given below:

$$\xi_{1,2} = \frac{\mu \cos \lambda \mp \cos \theta_n \sin \lambda}{\cos \theta_n \cos \lambda \pm \mu \sin \lambda} \tag{A1}$$

$$J_{1,2} = \frac{\frac{d^2}{4} \cdot \tan \lambda \cdot \xi_{1,2} \cdot m}{1 \pm \mu \cdot \xi_{1,2}} \tag{A2}$$

$$C_{1,2} = \frac{\frac{d}{2} \cdot \xi_{1,2}}{1 \pm \mu \cdot \xi_{1,2}} \tag{A3}$$

REFERENCES

[1] R.F. *ff.* Weir and D.S. Childress, *Encyclopedia of Applied Physics,* vol. 15, 1996, pp.115-140.
[2] D.S. Childress, *Atlas Limb Prosthetics, Surgical, Prosthetic, & Rehabilitation Principles*, 2nd ed., Bowker & Michael (Eds), Mosby-Year Book, 1992, pp. 175-199.
[3] R. F. *ff.* Weir, "Design of Artificial Arms and Hands for Prosthetic Applications" Invited Chapter (Chapter 32) in *Standard Handbook of Biomedical Engineering & Design,* Myer Kutz, Editor, McGraw-Hill, New York, 2003, pp. 32.1 – 32.61.
[4] Simpson, D.C., "The Choice of Control System for multimovement prostheses: Extended Physiological Proprioception (EPP)" in: *Control of Upper-Extremity Prostheses & Orthoses,* P. Herberts et al. (Eds), C.C. Thomas, 1974, pp. 146-150.
[5] J.A. Doubler and D.S. Childress, "Design and Evaluation of a Prosthesis Control System Based in the Concept of Extended Physiological Proprioception", *J. Rehabil. Res. Dev.*, vol. 21, pt1 pp. 5-18, pt2 pp. 19-31 1984.
[6] G. Vanghetti "Amputazioni, Disarticolozioni e protesi", Florence, Italy 1898.
[7] G. Vanghetti "Plastica dei Monconi a Scopo di Protesi Cinematica", *Arch. d. Ortop.,* Vol. 16, no. 5, 1899a, pp. 305-324.
[8] G. Vanghetti "Plastica dei Monconi a Scopo di Protesi Cinematica", *Arch. d. Ortop.,* Vol. 16, no. 6, 385-410 1899b.
[9] G. Vanghetti "Plastica dei Monconi ed Amputazioni Transitore", *Arch. d. Ortop.,* Vol. 17, no.5-6, 1900, pp. 305-329.
[10] F. Sauerbruch "Chirurgische Vorarbiet für eine Wilkürlich Bewegliche Künstliche Hand", *Mediziische Klinik,* Vol. 11, no. 41, 1915, pp. 1125-1126.
[11] F. Sauerbruch, "Die Wilkürlich Bewegbare Künstliche Hand" in *Eine Anleitung für Chirurgen und Techniker*, 1st ed. Berlin, Julius Springer-Verlag, 1916.
[12] P.E. Klopsteg and P.D. Wilson (Eds.), *Human Limbs and their substitutes,* 2nd ed., New York, McGraw-Hill, 1954.
[13] R.W. Beasley "Inter-Clinic Information Bulletin (ICIB)", New York, vol. 8, 1966, pp. 6-8.
[14] R.N. Scott, "Myoelectric Control of Prostheses a brief history", MEC 92, *Proceedings of the 1992 MyoElectric Controls/Powered Prosthetics Symposium*, Fredericton, New Brunswick, Canada, 1992.
[15] R.F. *ff.* Weir, C.W. Heckathorne, D.S. Childress, "Cineplasty as a control input for externally powered prosthetic components", *Journal of Rehabilitation Research & Development,* vol. 38, no 4, July/August 2001, pp. 357-363.
[16] D.S. Childress, E. Grahn, R.F. *ff.* Weir, C. Heckathorne and J. Uellendahl, "Modification of a Bock Hand for E.P.P. Control by Exteriorized Tendons", *Proceedings of the 19th Annual Meeting of AAOP,* 13, 1993.
[17] Y.A. Bertos, "A Microprocessor-based EPP Position Controller for Electric-Powered Upper-Limb Prostheses", MS Thesis, Northwestern University, Evanston, IL, USA, 1999.
[18] Y.A. Bertos, C.W. Heckathorne, R.F. *ff.* Weir and D.S. Childress, "Microprocessor Based E.P.P. Position Controller for Electric-Powered Upper-Limb Prostheses", *Proceedings of the 19th Annual International Conference of the IEEE-EMBS Society*, 1997, pp. 2311–2314.
[19] H.M Al-angari, R.F. *ff.* Weir, C.W. Heckathorne and D.S. Childress, "A two degree-of-freedom microprocessor based extended physiological proprioception (EPP) controller for upper limb prostheses", *Technology and Disability*, 15, IOS Press. 2003, pp. 113–127.
[20] R.C. Goertz, "Philosophy, development of manipulators", 1951 in *Teleoperated Robotics in hostile environments*, Martin, H.L., and Kuban, D.P. (editors), Society of Manufacturing Engineers, Dearborn, Michigan, 1985, pp. 257-262.
[21] R.C. Mosher, Handyman to Hardiman, SAE paper 67008*, Society of Automotive Engineers (SAE)*, Warrendale, PA, 1967.
[22] Y. Yokokohji and T. Yoshikawa, "Bilateral control of master-slave manipulators for ideal kinesthetic coupling-formulation and experiment," *IEEE Trans. on Robotics and Automation,* vol. 10, no. 5, 1994, pp. 605-620.
[23] Winters, J. M. and Stark, L. (1985a) "Analysis of fundamental movement patterns through the use of in-depth antagonistic muscle models." *IEEE Biomed. Engng.* BME-32, 826-839
[24] Winters, J. M. and Stark, L. "Estimated mechanical properties of synergistic muscles involved in movements of a variety of human joints." *J.Biomechanics* Vol.21, No. 12, pp. 1027-1041, 1988.
[25] Moutopoulou, E., Bertos, G.A., Mablekos-Alexiou, A., and Papadopoulos, E., "Feasibility of a Biomechatronic EPP Upper Limb Prosthesis Controller", *37th Annual International Conference of the IEEE Engineering in Medicine and Biology Society* (EMBS), 25-27 August 2015.